Protograph-Based LDPC Convolutional Codes for Continuous Phase Modulation

Tarik Benaddi*†‡, Charly Poulliat†‡,
Marie-Laure Boucheret †‡, Benjamin Gadat§ and Guy Lesthievent*
*CNES †University of Toulouse, ENSEEIHT/IRIT ‡TéSA - Toulouse §Thales Alenia Space

***Abstract*—The spatial coupling is an efficient technique that improves the threshold of Low Density Parity Check (LDPC) codes. In this paper, we investigate the performance of the serial concatenation of Continuous phase modulation (CPM) and LDPC convolutional codes over a memoryless additive white Gaussian noise channel. We show that coupling protographs optimized for CPM improves their performance and helps designing very good 'small' protographs. Inspired from convolutional codes and thanks to the inner structure of CPM, we also introduce a new termination without rate loss but that still exhibits a coupling gain and it thus has a very good threshold. We will illustrate the behavior of different LDPC convolutional codes with different termination methods by giving some examples and studying their performance using multidimensional EXIT analysis.**

***Keywords*—CPM, LDPC convolutional codes, termination, EXIT Chart, code design, iterative decoding**

I. Introduction

Continuous phase modulation (CPM) is a class of nonlinear phase modulation where the phase values are preserved continuous from one symbol interval to the other. Thanks to its constant envelope property, it is traditionally used with embedded amplifiers that operate near the saturation regime and in channel subject to nonlinearities. Because of its interesting properties, CPM is considered with cyclic interest as a good trade-off for different constraint wireless communication systems (satellite video broadcasting, bluetooth, telemetry mesures, GSM mobile network...). In particular, it is envisioned as a possible waveform for UAV aeronautical communications. CPM signal decoding is usually performed using the MAP algorithm over the CPM trellis [1]. This method results in relatively high complexity which restricts the use to some limited schemes (Minimum Shift Keying (MSK), Gaussian MSK (GMSK), continuous phase frequency shift keying CPFSK, ...). Then [2] shows that the CPM modulator can actually be seen as a time-invariant continuous phase encoder (CPE) concatenated with a time-invariant memoryless modulator (MM). Taking advantage of this decomposition, CPM has greatly benefited from the concept of turbo-decoding. Several papers considered serial concatenations with convolutional codes [3]–[6] and Low Density Parity Check (LDPC) codes [7]–[11].

The convolutional counterparts of LDPC codes are called LDPC convolutional (LDPC-C) codes [12]. They are part of a more general family often referred to as spatially coupled LDPC codes. LDPC-C codes are obtained by spatial coupling of LDPC block codes and can be defined also by a sparse parity check matrix which makes them adapted for message passing decoding. The coupling is an efficient technique that leads to substantially better thresholds even with relatively simple protographs under belief propagation (BP) in comparison to its LDPC block counterparts. Since their introduction, there are numerous papers on the analysis of their performance and on the reasons why they perform so good in comparison to classical LDPC codes over the BEC or Gaussian channel (see [13]–[15] and therein references for more details). Different methods have been proposed to construct LDPC-C codes. In this paper we will consider protograph-based LDPC convolutional codes.

To our knowledge, no work has been done to design and analyze the performance of LDPC-C codes concatenated with a CPM. In [16], the authors compared the performance of some LDPC-C codes over the Gaussian channel, proposed a $3/4 - rate$ universally good (with any mapping/MIMO detector) LDPC-C code candidate and illustrated it with the $16 - QAM$ receiver with different mappings. [17] showed that LDPC-C codes achieve the symmetric achievable rate for intersymbol-interference channels. For bit-interleaved coded modulations, [18] studied the performance of the LDPC-C codes and the optimization of the mapping where each bit channel is modeled by an independent binary erasure channel.

In this paper, we will see that, due to the inner structure of CPM, good codes for Gaussian channel do not exhibit necessarily good performance with CPM. We investigate the performance of the concatenated scheme formed by the serial concatenation of a LDPC-C code and a general CPM modulation scheme. We focus on finding LDPC-C codes that are good for a particular CPM modulator. We also show that coupling protographs that behave well with a particular CPM improves their threshold. Finally, we will show that we can adapt an unusual LDPC-C termination without rate loss but still having a very good threshold. The organization of this paper is as follows: first Section II briefly describes the system model. Section III is dedicated to the convergence analysis method. Section IV discusses some aspects on the convergence behavior of different codes and

shows some simulation results. Finally, based on these insights, Section V concludes the paper.

II. System description

We consider a concatenated scheme composed of a binary LDPC convolutional code serially concatenated with CPM modulator. A binary LDPC convolutional code can be described as the ensemble of codewords $\boldsymbol{c}_{[\mathbf{0},\boldsymbol{\infty}]} = \{c_0, c_1, ..., c_t, ...\}$, $c_t \in GF(2)$, that satisfy the equation $\boldsymbol{c}_{[\mathbf{0},\boldsymbol{\infty}]}\boldsymbol{B}^T_{[0,\infty]} = \mathbf{0}$, where $\boldsymbol{B}^T_{[0,\infty]}$ has the form:

$$\begin{bmatrix} \boldsymbol{B}_0^T(0) & \cdots & \boldsymbol{B}_{m_s}^T(m_s) & & & \\ & \ddots & & \ddots & & \\ & & \boldsymbol{B}_0^T(t) & \cdots & \boldsymbol{B}_{m_s}^T(t+m_s) & \\ & & & \ddots & & \ddots \end{bmatrix}$$

$\boldsymbol{B}^T_{[0,\infty]}$ is called the syndrome former of the code, $\{\boldsymbol{B}_i(t)\}_i$ the component matrices, m_s the syndrome former memory and $v_s = (m_s + 1)$ the constraint length. A more detailed definition can be found in [12].

A *protograph* [19] is a relatively small bipartite graph described by (V, C, E) where the set of variable nodes V (of cardinality v) is connected to the set of check nodes C (of cardinality c) through edges E. It can be described by its base matrix $\boldsymbol{B}$ where $B(r, s) \geq 0$ is the number of edges between the variable node (VN) s and the check node (CN) r. A protograph-based LDPC-C code can then be obtained by the edge spreading rule (ESR, [20]) applied to the base matrix B: the graph is replicated an infinite number of times, then each VNs bundle is connected to its pairing CNs bundle through a permutation of the corresponding edges bundle only in the forward direction, *i.e.* from the protograph at time t to the protographs at time $t' > t$. These connections are described by the components base matrices $\{\boldsymbol{B}_i\}_i$ which must satisfy:

$$\sum_{i=0}^{i=m_s} \boldsymbol{B}_i = \boldsymbol{B}$$

In this class of LDPC-C codes, the design rate of the base matrix can be written as $R = 1 - c/v$. Figure 1 shows an example of ESR operation corresponding to the base matrix $\boldsymbol{B} = [3 \quad 3]$.

In this paper we will consider mainly terminated time invariant LDPC convolutional codes [14]. They can be described by mean of convolutional protograph with the base matrix $\boldsymbol{B}_{[0,L-1]}$ of size $(L + m_s)c \times Lv$. In this case, L is called the termination factor or the coupling length.

$$\boldsymbol{B}^T_{[0,L-1]} = \begin{bmatrix} \boldsymbol{B}_0^T & \cdots & \boldsymbol{B}_{m_s}^T & & \\ & \ddots & & \ddots & \\ & & \boldsymbol{B}_0^T & \cdots & \boldsymbol{B}_{m_s}^T \end{bmatrix} \quad (1)$$

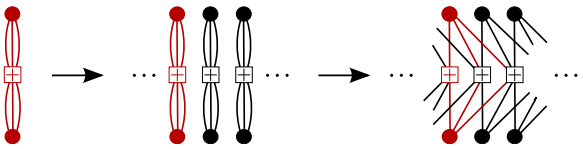

Fig. 1: (3, 6) regular LDPC convolutional code with $m_s = 2$: firstly, the protograph is replicated, then it is spatially coupled with respect to $\boldsymbol{B_0} = \boldsymbol{B_1} = \boldsymbol{B_2} = [1 \quad 1]$

The design rate of terminated LDPC-C codes without puncturing becomes:

$$R_L = 1 - \frac{(L + m_s)}{L}(1 - R) = R - \frac{m_s}{L}(1 - R) \quad (2)$$

One should observe that the termination as shown in Eq. (1) results in a rate loss by a penalty of $\frac{m_s}{L}(1-R)$ as depicted by Eq. (2). Note that, as L increases, R_L increases and approaches the design rate R, and the singularity in the code profile introduced by the firsts and lasts check nodes (less connected) becomes minor. At the decoder side, we consider BP decoding algorithm [21].

Each codeword $\boldsymbol{c}_{[\mathbf{0},\boldsymbol{L-1}]}$ is interleaved, mapped into M-ary symbols $\boldsymbol{\alpha} = \{\alpha_i\}_i$, where $\alpha_i \in \{\pm 1, ..., \pm(M-1)\}$, and encoded by the CPM modulator. The normalized complex baseband CPM signal can be written as:

$$s(t, \boldsymbol{\alpha}) = \exp j\theta(t, \boldsymbol{\alpha}) \quad (3)$$

with:

$$\theta(t, \boldsymbol{\alpha}) = 2\pi h \sum_{i=0}^{N-1} \alpha_i q(t - iT), q(t) = \begin{cases} \int_0^t g(\tau)d\tau \\ 1/2, t > L_{cpm} \end{cases}$$

$\theta(t, \boldsymbol{\alpha})$ the information carrying phase, $g(t)$ the frequency pulse, $h = k/p$ the modulation index and L_{cpm} the memory. Practically, the shape of $q(t)$ (rectangular (REC), raised-cosine (RC), ...) and L_{cpm} determine the smoothness of the phase transitions. If $L_{cpm} = 1$, we say that we have a full response waveform, otherwise, if $L_{cpm} > 1$, a partial response waveform. For GMSK, the modulation choosed for GSM system, $h = 1/2$, $L_{cpm} = 3$, $M = 2$, $BT = 0.3$, and the pulse response is a Gaussian.

Let $U_i = (\alpha_i + (M - 1))/2 \in \{0, 1, ..., M - 1\}$. According to [2], the CPM modulator can be represented by the concatenation of a continuous phase encoder (CPE), described as a time invariant trellis defined by the tuple $\sigma_n = [U_{n-1}, ..., U_{n-L+1}, [\sum_{i=0}^{n-L} U_i] mod\ p]$, followed by a memoryless modulator (MM), formed by pM^L different filters $\{s_i(t)\}$ corresponding to CPE output symbols $X_n = [U_n, ..., U_{n-L+1}, [\sum_{i=0}^{n-L} U_i] mod\ p]$.

We assume here that the transmitted signal $s(t, \boldsymbol{\alpha})$ is sent over a memoryless additive white Gaussian noise (AWGN) channel having a double-sided power spectral density $N_0/2$. From Eq. (3), the received signal has the complex baseband expression:

$$y(t) = \sqrt{2E_s/T} exp\{j\psi(t, \boldsymbol{\alpha})\} + n(t)\ ,\ t > 0 \quad (4)$$

where $\psi(t, \boldsymbol{\alpha})$ is the tilted phase [2]. The outputs of the MM filters at the receiver are sampled once each T to form the projections of the received signal $\boldsymbol{y^n} = [y_i^n = \int_{nT}^{(n+1)T} y(l)s_i^*(l)dl]_{1\leq i\leq pM^{L_{cpm}}}$. Considering any orthogonal basis of the receiver signal space [3], $p(\boldsymbol{y^n}/X_n)$ can be simplified to $\exp\{2Re(y_i^n)/N_0\}$. This metric is for the transitions of the CPE trellis when running the BCJR algorithm [22].

Fig. 2 depicts the receiver considered in this paper. The copy-and-permute operation (called also lifting) of the convolutional protograph is done by replacing each node with a bundle of node of the same type and replacing each edge with the bundle of a permutation of edges of the same type.

III. Asymptotic Convergence analysis

In this section, we will study the asymptotic convergence for the AWGN channel for different protograph-based LDPC-C codes. We consider the following scheduling: an iteration ℓ consists in one BCJR forward backward recursion for the CPM soft decoder, followed by one BP data pass check pass for the LDPC-C code. We further assume partial interleavers between the CPM module and each VN bundle [11], [23].

Using density evolution techniques to determine the threshold of the generalized CPM scheme concatenated with different LDPC-C for the AWGN channel is a prohibitive task. Instead, we will use EXIT chart analysis [24]. It tracks the variance σ_{llr}^2 (or the mean m_{llr}) of exchanged log likelihood ratios (LLR) under consistent Gaussian distributed messages ($m_{llr} = \sigma_{llr}^2/2$) and reciprocal channel approximations using the monodimensional function of σ_{llr}^2 noted $J(.)$ [25]:

$$J(\sigma_{llr}^2) := 1 - E_x(log_2(1 + e^{-x})), x \sim \mathcal{N}(\frac{\sigma_{llr}^2}{2}, \sigma_{llr}^2)$$

While EXIT analysis works fine for LDPC codes, this method is not accurate when coming accros protograph-based codes. Actually, [26] proved that because of the relatively small size and the lifting operation which introduces an inherent structure within the corresponding LDPC code, classical EXIT charts cannot predict accurately the threshold (the minimum channel parameter that ensures reliable decoding). Instead, we will use protograph or multidimentinal EXIT charts [26]. Let us consider hereafter the following notations relative to the ℓ^{th} iteration:

- $I_v^\ell(q, r)$: extrinsic mutual information (eMI) between the code bits associated with VN r and the LLRs sent from this VN to the CN q.
- $I_c^\ell(q, r)$: eMI associated with messages sent from CN q to VN r.
- $I_{app}^\ell(r)$: *a posteriori* MI associated with the VN r.
- $I_{a,CPM}^\ell(r)$: *a priori* MI associated with messages sent from the VN r to the CPM soft decoder.
- $I_{CPM}^\ell(r)$: eMI associated with messages sent from CPM soft decoder to the VN r.
- $T_{CPM}(.)$: input-output EXIT transfer function of the CPM detector implicitly depending the noise variance σ_{noise}^2. Analytic expression is not straightforward, but it can be evaluated with Monte Carlo simulations.

Let us consider a mother protograph B, of size $c \times v$, which generates the terminated LDPC-C code $B_{[0,L-1]}$ of size $Lv \times (L + m_s)c$, noted hereafter B_L for ease of notations. The CPM update equations at iteration ℓ seen by the variable node r are given by:

$$I_{CPM}^\ell(r) = T_{CPM}(I_{a,CPM}^{\ell-1}(r)) \tag{5}$$

$$I_{a,CPM}^\ell(r) = J\left(\sqrt{\sum_s B_L(s,r)\left[J^{-1}(I_v^{\ell-1}(s,r))\right]^2}\right) \tag{6}$$

When $B_L(q, r) \neq 0$, the VN r to CN q update equation is formally given by:

$$I_v^\ell(q,r) = J\left(\sqrt{\sum_s B_L(s,r)\left[J^{-1}(I_c^{\ell-1}(s,r))\right]^2 - \left[J^{-1}(I_c^{\ell-1}(q,r))\right]^2 + \left[J^{-1}(I_{CPM}^\ell(r))\right]^2}\right) \tag{7}$$

otherwise, $I_v^\ell(q, r) = 0$. Similarly, using reciprocal channel approximation, CN q to VN r update is given by:

$$I_c^\ell(q,r) = 1 - J\left(\sqrt{\sum_s B_L(q,s)\left[J^{-1}(1 - I_v^\ell(q,s))\right]^2 - \left[J^{-1}(1 - I_v^\ell(q,r))\right]^2}\right) \tag{8}$$

otherwise, $I_c^\ell(q, r) = 0$.

Considering partial interleavers [11], at the end of each iteration, the *a posteriori* MI evaluated at the VN r is:

$$I_{app}^\ell(r) = J\left(\sqrt{\sum_s B_L(s,r)\left[J^{-1}(I_c^{\ell-1}(s,r))\right]^2 + \left[J^{-1}(I_{CPM}^\ell(r))\right]^2}\right) \tag{9}$$

Combining Eqs. (5) to (9), we can track the evolution of I_{app}^ℓ for each VN through iterations. The threshold is defined as the smallest E_b/N_0 such that for all r, $I_{app}^\ell(r) = 1$ after a certain number of iterations ℓ.

IV. Code design and optimization

We are interested here by finite length block codes, *i.e.* the LDPC-C codes with finite L.

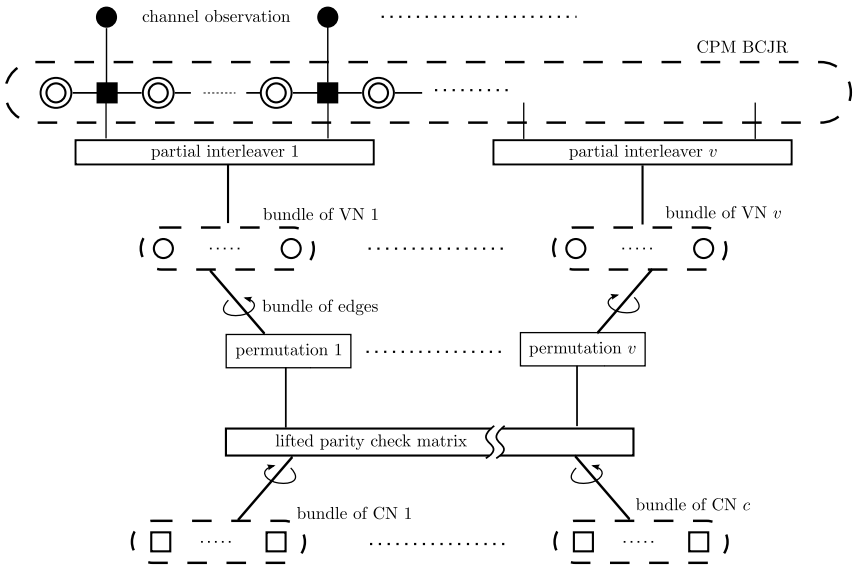

Fig. 2: Factor graph of the receiver.

A. Classical methods for protograph construction

As for convolutional codes, there are two main methods to terminate LDPC-C codes:

Termination (T): If the LDPC-C code in interpreted from its base matrix B_L, T termination is equivalent to truncating all VNs of $B_{[0,\infty]}$ after the L^{th} copy as in Fig. 1, and keeps only the CNs that are connected up to the L^{th} stage of VNs.

Tail-bitting (TB): In order to avoid the rate loss, tail-bitting method has been introduced [27]. The corresponding parity check matrix B_L^{tb} can be found in [28]. Because the most right-hand and left-hand CNs are no more 'irregular', there is no coupling gain with this familly and the threshold will remain the same as for the underlying protograph B. However, since the CNs and VNs profiles remain unchanged in comparison to the mother protograph, TB LDPC-C codes are used generally to obtain some bounds (free distance, trapping set, ...) of the T termination LDPC-C codes [27].

As already pointed out, the iterative decoding threshold improvement gained with LDPC-C codes in comparison to the unstructured LDPC codes is due the *wave effect* induced by check nodes (less connected degree check nodes). This phenomenon is depicted in Fig. 3a: the less connected check nodes generated more reliable LLRs, which, as iterations go along, gradually propagates from both sides to internal nodes. For the middle VNs, as far as the wave effect did not affect them yet, behave roughly the same way as the VNs of the base protograph B. If E_b/N_0 is larger than the threshold of B_L (which is lower than the threshold of B), the decoding wave is strong enough to make them converge as depicted in Fig. 3b. As said before, the advantage of TB termination is to insure the same rate as B. However, since the edges CNs are no more irregular, properties of B are conserved (same rate and threshold) as depicted in Fig. 3c.

B. New method: direct truncation

In this section, we introduce a new protograph based LDPC-C code termination that we believe is interesting for some concatenated schemes. Similarly to convolutional codes [29], one can suggest to consider a direct truncation (DT) for the LDPC-C code. It is constructed like tailbitting LDPC-C, but instead of adding $m_s c$ CNs at the right-hand end to satisfy L^{th} set of VNs connections, we remove all unconnected edges. The main advantage is the conservation of the rate $R_{DT} = R$. The parity check matrix is written as:

$$\boldsymbol{B}_L^{DT} = \begin{bmatrix} \boldsymbol{B}_0 & & & \\ \vdots & \boldsymbol{B}_0 & & \\ \boldsymbol{B}_{m_s} & \vdots & \ddots & \\ & \boldsymbol{B}_{m_s} & \dots & \boldsymbol{B}_0 \end{bmatrix} \tag{10}$$

It is obvious that the left-hand nodes configuration did not change, compared to B_L, which means that the convolutional gain induced by these nodes is preserved. On the contrary, the most right-hand nodes, a small proportion of poorly connected VNs is introduced while previous poorly connected CNs disappears. The direct effect of these VNs is that they will converge slowly in comparison to their counterparts in B_L: which means that the corresponding bits have less error protection in comparison to other bits. Besides that, one would say that having at least one $degree - 1$ VNs among the last v VNs may hurt the convergence. Actually, by choosing a good coupling component matrices, not only the proportion of these tedious VNs vanishes with increasing L, but also their effect is surprisingly alleviated by both the coupling gain and the fact that, unlike other modulations, usual CPM schemes have EXIT curves that converge to the point $(1, 1)$ [23].

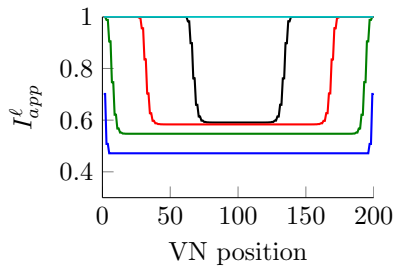

(a) T, R=0.49, E_b/N_0=3.1dB, iterations $\{1, 5, 20, 60, 63\}$.

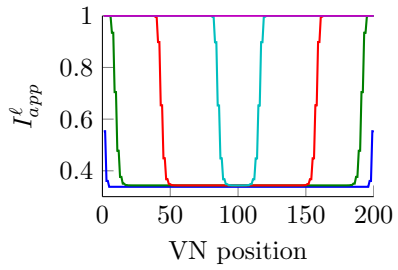

(b) T, R=0.49, E_b/N_0=1.1dB, iterations $\{1, 20, 100, 200, 235\}$.

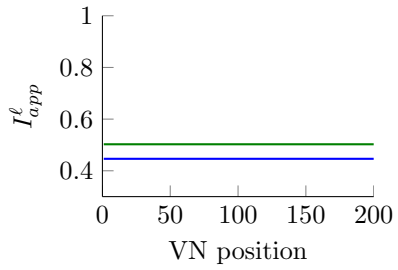

(c) TB, R=0.5, E_b/N_0=2.1dB, iterations $\{1, 1000\}$.

Fig. 3: Evolution of I^{ℓ}_{app} per variable nodes of the LDPC-C depicted in Fig. 1 concatenated with GMSK, $L = 100$. threshold of B is 2.22dB

C. Design examples

As an example, we consider the following codes:

- $C^{(1)}$: $(3, 6) - regular$ protograph
- $C^{(2)}$: protograph proposed in [11]
- $C^{(1)}_{1,T}$: coupling of $C^{(1)}$ with m_s=1
  $\boldsymbol{B_0^{(1)}} = [1\ 2]$ and $\boldsymbol{B_1^{(1)}} = [2\ 1]$
- $C^{(1)}_{1,DT}$: direct truncation of $C^{(1)}_{1,T}$
- $C^{(1)}_{2,T}$: coupling of $C^{(1)}$ with m_s=2
  $\boldsymbol{B_0^{(2)}} = \boldsymbol{B_1^{(2)}} = \boldsymbol{B_2^{(2)}} = [1\ 1]$
- $C^{(1)}_{2,DT}$: direct truncation of $C^{(1)}_{2,T}$
- $C^{(2)}_{1,T}$: coupling of $C^{(2)}$ with m_s=1 and:

$$\boldsymbol{B_0} = \begin{bmatrix} 1 & 1 & 0 & 0 & 1 & 1 & 0 & 0 \\ 0 & 1 & 0 & 0 & 0 & 0 & 1 & 0 \\ 1 & 1 & 1 & 0 & 0 & 0 & 0 & 1 \\ 0 & 0 & 0 & 0 & 0 & 0 & 0 & 0 \end{bmatrix}$$

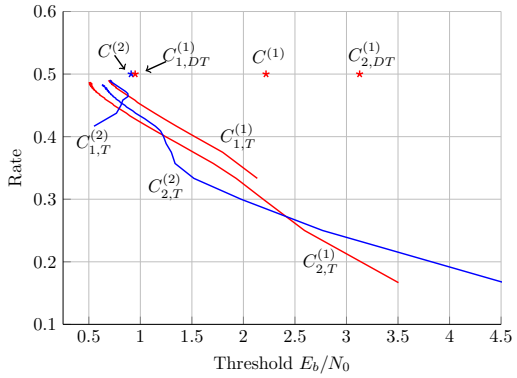

Fig. 4: Thresholds comparison for different codes when GMSK

$$\boldsymbol{B_1} = \begin{bmatrix} 0 & 0 & 0 & 0 & 0 & 0 & 0 & 0 \\ 1 & 1 & 0 & 1 & 0 & 1 & 0 & 0 \\ 1 & 0 & 0 & 0 & 0 & 0 & 1 & 0 \\ 1 & 1 & 0 & 0 & 0 & 0 & 0 & 1 \end{bmatrix}$$

- $C^{(2)}_{2,T}$: coupling of $C^{(2)}$ with m_s=2 and:

$$\boldsymbol{B_0} = \begin{bmatrix} 0 & 1 & 0 & 0 & 0 & 1 & 0 & 0 \\ 0 & 1 & 0 & 0 & 0 & 0 & 0 & 0 \\ 0 & 0 & 1 & 0 & 0 & 0 & 0 & 0 \\ 1 & 0 & 0 & 0 & 0 & 0 & 0 & 0 \end{bmatrix}$$

$$\boldsymbol{B_1} = \begin{bmatrix} 1 & 0 & 0 & 0 & 0 & 0 & 0 & 0 \\ 1 & 1 & 0 & 0 & 0 & 1 & 0 & 0 \\ 0 & 0 & 0 & 0 & 0 & 0 & 1 & 0 \\ 0 & 0 & 0 & 0 & 0 & 0 & 0 & 1 \end{bmatrix}$$

$$\boldsymbol{B_1} = \begin{bmatrix} 0 & 0 & 0 & 0 & 1 & 0 & 0 & 0 \\ 0 & 0 & 0 & 1 & 0 & 0 & 1 & 0 \\ 2 & 1 & 0 & 0 & 0 & 0 & 0 & 1 \\ 0 & 1 & 0 & 0 & 0 & 0 & 0 & 0 \end{bmatrix}$$

Figure 4 depicts the decoding thresholds for the above codes with GMSK modulation as a function of L. We observe that with increasing L, the design rate R_L for $C^{(1)}_{1,T}$, $C^{(1)}_{2,T}$, $C^{(2)}_{1,T}$ and $C^{(2)}_{2,T}$ converges to R. Notice that the coupling has significantly improved the thresholds of $C^{(1)}$ and $C^{(2)}$. Concerning our termination method, the spatial coupling of the $(3, 6) - regular$ code with respect to $\{B^{(2)}_i\}$, *i.e.* $C^{(1)}_{2,DT}$, drastically decreases the threshold. On the contrary, the direct truncation of the spatial coupling following $\{B^{(1)}_i\}$, *i.e.* $C^{(1)}_{1,DT}$, the DT method allows us to obtain directly a code with rate R and that has some advantages for encoding. These advantages come with a very small degradation of the threshold. If one want to design convolutional protograph that behave very good with both T and DT terminations, $C^{(1)}_{1,DT}$ is a very good candidate.

The VNs convergence for $C^{(1)}_{1,DT}$ and $C^{(1)}_{2,DT}$ are visualized in Fig. 5 at 1.5dB. Notice that the wave effect travels only from the left side to the right side, because of the less connected CNs present at the first rows. Recall that the $C^{(1)}$ threshold is only $E_b/N_0 = 2.2$dB (> 1.5dB), consequently, the middle VNs, which behave as the VNs of $C^{(1)}$, do not converge through iterations and wait for the wave gain. For $C^{(1)}_{1,DT}$ (resp. $C^{(1)}_{2,DT}$), on the most right hand VNs, we recognize, as expected, a small degradation

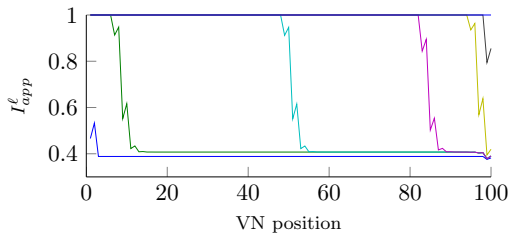

(a) $C^{(1)}_{1,DT}$, iterations {1, 20, 120, 200, 230, 240, 250}. Convergence of all VNs after 250 iterations

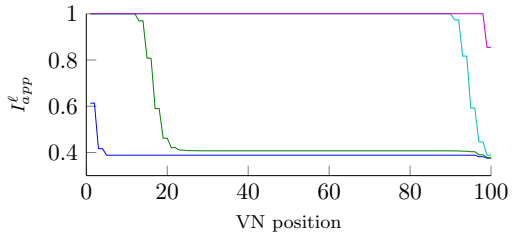

(b) $C^{(1)}_{2,DT}$, iterations {1, 20, 120, 200, 1000}. Curves of the 200^{th} and the 1000^{th} iterations are overlaid

Fig. 5: Evolution of I^{ℓ}_{app} per VNs of $C^{(1)}_{1,DT}$ and $C^{(1)}_{2,DT}$, with $L = 50$, concatenated with GMSK at 1.5dB

because of the less connected VNs (corresponding to the last columns of the parity check matrix) whose connections are fully determined only by $\boldsymbol{B}^{(1)}_{\mathbf{0}}$ (resp. $\boldsymbol{B}^{(2)}_{\mathbf{0}}$), $\forall L$. On the contrary of $C^{(1)}_{1,DT}$, the wave effect in $C^{(1)}_{2,DT}$ is not strong enough to make the last two $degree - 1$ deficient VNs converge. On the other hand, even if the coupling of $C^{(1)}$ (through $\{\boldsymbol{B}^{(1)}_{\boldsymbol{i}}\}$) leads to a slightly worse performance than the coupling of $C^{(2)}$ (through $\{\boldsymbol{B}^{(2)}_{\boldsymbol{i}}\}$) for the classical termination (T) (0.2dB), it is best suited to our no-rateless termination (DT) $C^{(3)}$ (which shows a degradation of the threshold of only 0.25dB).

For the protographs designed for the GMSK, the two proposed couplings, $C^{(2)}_{1,T}$ and $C^{(2)}_{2,T}$, show a gain of 0.2dB and 0.3dB respectively over $C^{(2)}$ (if we neglect the small rate loss at high values of L). Because $C^{(2)}$ is optimized for the GMSK, it already presents a good threshold and the spatially coupling operation did not show a large gain as when coupling spatially $C^{(1)}$. Furthermore, at high rates, at equal syndrome former memory m_s, the proposed LDPC-C codes corresponding to both $C^{(1)}$ and $C^{(2)}$ offer approximately the same performance, however, $C^{(2)}_{1,T}$ shows the best trade-off between the rate penalty (at most, when L is small, the gap to 0.5 is only of 0.18) and the threshold (varies between 0.55dB and 0.68dB) for the whole range of values of L. Small values of L, *i.e.* that lead to convolutional protographs with small size, are particularly interesting for finite length design. From this perspective, the performance of the proposed codes is depicted in Fig. 6: threshold is plotted as a function of the total number of VNs for different rate families. When we impose relatively strict constraints on the rateloss, the code which exhibits the best trade-off between threshold and

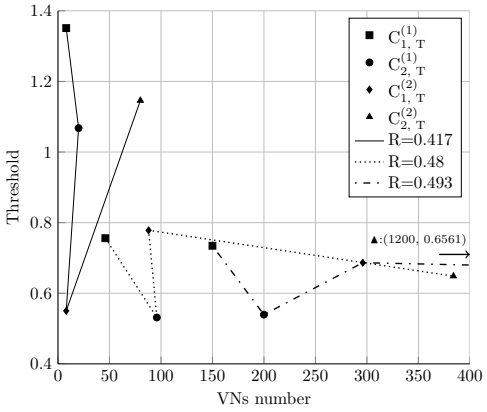

Fig. 6: Comparison of the threshold as a function of the number of VNs for different rates

	$C^{(1)}$	$C^{(2)}$	$C^{(1)}_{1,T}$	$C^{(1)}_{1,DT}$
Threshold	2.84	1.38	1.13	1.13
Rate	0.5	0.5	0.495	0.5

$C^{(1)}_{2,T}$	$C^{(1)}_{2,DT}$	$C^{(2)}_{1,T}$	$C^{(2)}_{2,T}$
0.82	3.15	0.97	0.93
0.49	0.5	0.49	0.48

TABLE I: Comparison of the performance of some codes when concatenated with Q_{CPM}

protograph size, when the rateloss is of about 0.007, is $C^{(1)}_{2,T}$. On the other hand, when we tolerate a rateloss of 0.083, it is clear that $C^{(2)}_{1,T}$ outperforms all other proposed codes.

For quaternary CPM, Table I summarizes some results. For ease of presentation, we compare the codes with coupling factor $L = 50$ when concatenated with the CPM modulator Q_{CPM}: quaternary, Gray mapping, $L_{CPM} = 2$, Raised cosine pulse and $h = 1/4$. Concerning the optimized protograph codes, $C^{(2)}$ still have a very good performance [11]. The performance one can achieve when optimizing rate-1/2 unstructured LDPC codes for this CPM is 0.7dB [11], here we almost achieved this limit with $C^{(2)}_{1,T}$ As for the binary case, similar observations can be made, however, the direct truncation $C^{(1)}_{1,DT}$ clearly leads here to better performance in comparison to the classical termination $C^{(1)}_{1,T}$, since both have the same threshold (1.13dB) while the latter has a worse rate.

Figure 7 gives some simulation results for $C^{(2)}$ and $C^{(2)}_{1,T}$ when concatenated with GMSK. Simulation were performed using 250 turbo iterations and a lifting factor of around 1000. For the spatially coupled code, we take $L = 50$.

V. CONCLUSION

In this paper, we have investigated the performance and the convergence behavior of some LDPC-C codes when concatenated with CPM. We show that coupling protographs optimized for CPM improves their performance and helps designing very good small protographs. Furthermore, we described

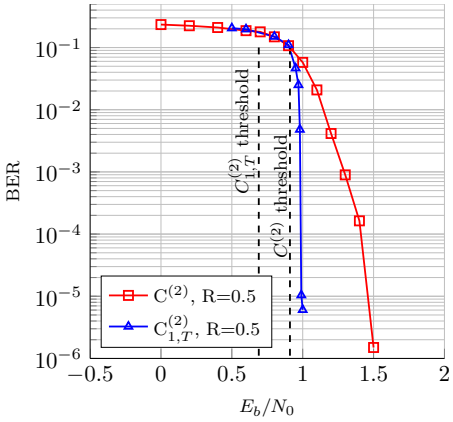

Fig. 7: Bit error rate for GMSK with different codes

an unusual termination without rate loss that still has a good threshold. Nonetheless, the gain of our termination should come with a degradation of the growth rate, future works will investigate this aspect. Also, for CPM of high modulation orders, bit interleaved coded CPM approach can be considered to explore the optimization of the bit mapping to alleviate the threshold penalty of DT termination.

REFERENCES

[1] John B Anderson, Tor Aulin, and Carl-Erik Sundberg, *Digital phase modulation*, Springer, 1986.

[2] Bixio E Rimoldi, "A decomposition approach to cpm," *IEEE Trans. Inf. Theory*, vol. 34, no. 2, pp. 260–270, 1988.

[3] Pär Moqvist and Tor M Aulin, "Serially concatenated continuous phase modulation with iterative decoding," *IEEE Trans. Commun.*, vol. 49, no. 11, pp. 1901–1915, 2001.

[4] Krishna R Narayanan and Gordon L Stuber, "A serial concatenation approach to iterative demodulation and decoding," *IEEE Trans. Commun.*, vol. 47, no. 7, pp. 956–961, 1999.

[5] Alexandre Graell i Amat, Charbel Abdel Nour, and Catherine Douillard, "Serially concatenated continuous phase modulation for satellite communications," *IEEE Trans. Wireless Commun*, vol. 8, no. 6, pp. 3260–3269, 2009.

[6] R Chaggara, ML Boucheret, C Bazile, E Bouisson, A Ducasse, and JD Gayrard, "Continuous phase modulation for future satellite communication systems in ka band," in *2004 International Conference on Information and Communication Technologies: From Theory to Applications, 2004. Proceedings.* IEEE, 2004, pp. 269–270.

[7] Krishna R Narayanan, Ibrahim Altunbas, and R Sekhar Narayanaswami, "Design of serial concatenated msk schemes based on density evolution," *IEEE Trans. Commun.*, vol. 51, no. 8, pp. 1283–1295, 2003.

[8] Krishna R Narayanan, Ibrahim Altunbas, and R Narayanaswami, "On the design of ldpc codes for msk," in *IEEE Global Telecommunications Conference, 2001. GLOBECOM'01.* IEEE, 2001, vol. 2, pp. 1011–1015.

[9] Aravind Ganesan, *Capacity estimation and code design principles for continuous phase modulation (CPM)*, Ph.D. thesis, Texas A&M University, 2003.

[10] Ming Xiao and Tor Aulin, "Irregular repeat continuous phase modulation," *IEEE communications letters*, vol. 9, no. 8, pp. 722–725, 2005.

[11] Tarik Benaddi, Charly Poulliat, Marie-Laure Boucheret, Benjamin Gadat, and Guy Lesthievent, "Design of unstructured and protograph-based ldpc coded continuous phase modulation," in *2014 IEEE International Symposium on Information Theory (ISIT)*. IEEE, 2014, pp. 1982–1986.

[12] A Jimenez Felstrom and Kamil Sh Zigangirov, "Time-varying periodic convolutional codes with low-density parity-check matrix," *IEEE Trans. Inf. Theory*, vol. 45, no. 6, pp. 2181–2191, 1999.

[13] Shrinivas Kudekar, Thomas J Richardson, and Rüdiger L Urbanke, "Threshold saturation via spatial coupling: Why convolutional ldpc ensembles perform so well over the bec," *IEEE Trans. Inf. Theory*, vol. 57, no. 2, pp. 803–834, 2011.

[14] David GM Mitchell, Michael Lentmaier, and Daniel J Costello, "Awgn channel analysis of terminated ldpc convolutional codes," in *Information Theory and Applications Workshop (ITA), 2011*. IEEE, 2011, pp. 1–5.

[15] Shrinivas Kudekar, Tom Richardson, and Rüdiger Urbanke, "Spatially coupled ensembles universally achieve capacity under belief propagation," in *2012 IEEE International Symposium on Information Theory Proceedings (ISIT)*. IEEE, 2012, pp. 453–457.

[16] Laurent Schmalen and Stephan ten Brink, "Combining spatially coupled ldpc codes with modulation and detection," in *Proceedings of 2013 9th International ITG Conference on Systems, Communication and Coding (SCC)*. VDE, 2013, pp. 1–6.

[17] Phong S Nguyen, Arvind Yedla, Henry D Pfister, and Krishna R Narayanan, "Spatially-coupled codes and threshold saturation on intersymbol-interference channels," *arXiv preprint arXiv:1107.3253*, 2011.

[18] Christian Häger, Alex Alvarado, Fredrik Brännström, Erik Agrell, et al., "Optimized bit mappings for spatially coupled ldpc codes over parallel binary erasure channels," *arXiv preprint arXiv:1309.7583*, 2013.

[19] JC Thorpe, "Low-density parity-checks codes (ldpc) constructed from protographs," *IPN Progress Report*, pp. 42–154, 2003.

[20] David GM Mitchell, Michael Lentmaier, and Daniel J Costello Jr, "Spatially coupled ldpc codes constructed from protographs," *arXiv preprint arXiv:1407.5366*, 2014.

[21] Thomas J Richardson and Rüdiger L Urbanke, "The capacity of low-density parity-check codes under message-passing decoding," *IEEE Trans. Inf. Theory*, vol. 47, no. 2, pp. 599–618, 2001.

[22] LR Bahl, J Cocke, F Jelinek, and J Raviv, "Optimal decoding of linear codes for minimizing symbol error rate (corresp.)," *IEEE Trans. Inf. Theory*, vol. 20, pp. 284–287, 1974.

[23] Tarik Benaddi, Charly Poulliat, Marie-Laure Boucheret, Benjamin Gadat, and Guy Lesthievent, "Design of systematic gira codes for cpm," *Proc. of ISTC*, 2014.

[24] Stephan Ten Brink, "Convergence behavior of iteratively decoded parallel concatenated codes," *IEEE Trans. Commun.*, vol. 49, no. 10, pp. 1727–1737, 2001.

[25] Stephan ten Brink, Gerhard Kramer, and Alexei Ashikhmin, "Design of low-density parity-check codes for modulation and detection," *IEEE Trans. Commun.*, vol. 52, no. 4, pp. 670–678, 2004.

[26] Gianluigi Liva and Marco Chiani, "Protograph ldpc codes design based on exit analysis," in *IEEE Global Telecommunications Conference, 2007. GLOBECOM'07*. IEEE, 2007, pp. 3250–3254.

[27] David GM Mitchell, Ali E Pusane, and Daniel J Costello, "Minimum distance and trapping set analysis of protograph-based ldpc convolutional codes," *IEEE Trans. Inf. Theory*, vol. 59, no. 1, pp. 254–281, 2013.

[28] Michael Lentmaier, David GM Mitchell, Gerhard Fettweis, and Daniel J Costello, "Asymptotically good ldpc convolutional codes with awgn channel thresholds close to the shannon limit," in *2010 6th International Symposium on Turbo Codes and Iterative Information Processing (ISTC)*. IEEE, 2010, pp. 324–328.

[29] Howard H Ma and Jack K Wolf, "On tail biting convolutional codes," *IEEE Trans. Commun.*, vol. 34, pp. 104–111, 1986.